J. Membrane Biol. 158, 219–228 (1997)

The Journal of
Membrane
Biology

Water Permeability of Brush Border Membrane Vesicles from Kidney Proximal Tubule

G. Soveral[1,3], R.I. Macey[4], T.F. Moura[1,2]

[1]Instituto de Tecnologia Química e Biológica (ITQB). Universidade Nova de Lisboa, Apartado 127, 2780 Oeiras, Portugal
[2]Dep. Química (and Centro de Química Fina e Biotecnologia), Faculdade de Ciências e Tecnologia, Universidade Nova de Lisboa, 2825 Monte da Caparica, Portugal
[3]Faculdade de Farmácia, Universidade de Lisboa, 1690 Lisboa, Portugal
[4]Department of Molecular and Cell Biology, University of California, Berkeley, CA 94720, USA

Received: 8 August 1996/Revised: 4 March 1997

Abstract. Brush border membrane vesicles (BBMV) maintain an initial hydrostatic pressure difference between the intra- and extravesicular medium, which causes membrane strain and surface area expansion (Soveral, Macey & Moura, 1997). This has not been taken into account in prior osmotic water permeability P_f evaluations. In this paper, we find further evidence for the pressure in the variation of stopped-flow light scattering traces with different vesicle preparations. Response to osmotic shock is used to estimate water permeability in BBMV prepared with buffers of different osmolarities (18 and 85 mosM). Data analysis includes the dissipation of both osmotic and hydrostatic pressure gradients. P_f values were of the order of 4×10^{-3} cm sec^{-1} independent of the osmolarity of the preparation buffer. Arrhenius plots of P_f *vs. 1/T* were linear, showing a single activation energy of 4.6 kcal mol^{-1}. The initial osmotic response which is significantly retarded is correlated with the period of elevated hydrostatic pressure. We interpret this as an inhibition of P_f caused by membrane strain and suggest how this inhibition may play a role in cell volume regulation in the proximal tubule.

Key words: Kidney vesicles — Brush border — Hydrostatic pressure — Water permeability — Volume regulation

Introduction

Brush border (BBMV) and basolateral membrane vesicles (BLMV) from kidney proximal tubule have been widely used in water transport experiments. The determination of permeability coefficients using these membrane preparations are advantageous because they are more resistant and viable than intact cells (Rigler, Ferreira & Patton, 1985; Donowitz et al., 1987), and because they permit the preparation of vesicles with any chosen internal media, expanding the range of experimental conditions. Further, studies of isolated vesicles allow the composite permeability of the whole cell to be split into its component parts and yield more precise information about driving forces and about the main route for water transport in the whole epithelia: transcellular or transjunctional.

The experimental evidence for the existence of protein water channels in RBC (Macey, 1984; Solomon, 1989) and in renal epithelia (Verkman, 1992) are based on high osmotic water permeability coefficients (P_f) inhibited by mercurial reagents, low activation energy, and the discrepancy between osmotic and diffusional permeability. High water permeability coefficients in BBMV from rat and rabbit kidney proximal tubule were reported (van der Goot, Podevin & Corman, 1989*a;* van der Goot, Ripoche & Corman, 1989*b;* van Heeswijk & van Os, 1986; Meyer & Verkman, 1987; Pratz, Ripoche & Corman, 1986). These P_f values were inhibited in the presence of the mercurial sulfhydryl reagents $HgCl_2$ and pCMBS, an effect reversed by cysteine addition.

Later studies revealed that a 28 KDa integral membrane protein, CHIP28, is the major erythrocyte water transporter, and provides an important route for water transport in proximal tubule and thin descending limb of Henle (Preston & Agre, 1991). These findings support a main transcellular pathway for water movement through renal epithelia.

Measurements of membrane osmotic permeability

Correspondence to: T.F. Moura[2]

(P_f), its inhibition by sulfhydryl reagents, and determination of the activation energy are often evaluated using a stopped-flow technique, where the time course of water flow that induces vesicular volume changes can be easily followed. A typical experimental approach, used to minimize the signal-to-noise ratio, consists in preparing the vesicles in low osmolarity buffers (20 to 60 mosM), in order to have larger volume changes at small gradients, a fact that slows down the time course of vesicular volume change (Meyer & Verkman, 1987; van der Goot et al., 1989*a;* van Hoek, Jong & van Os, 1990). We have found that vesicles prepared under these conditions maintain an initial hydrostatic pressure difference between the intra- and extavesicular medium, which causes membrane strain and surface area expansion (Soveral et al., 1997). This phenomena has not been taken into account in prior P_f evaluations. In this paper, we calculate P_f in BBMV prepared with buffers of different osmolarities (18 and 85 mosM), and use a method of analysis where the dissipation of both the osmotic and the hydrostatic pressure difference are considered. We find a slow initial osmotic response which is correlated with the period of elevated hydrostatic pressure and interpret this as an inhibition of P_f caused by membrane strain. Finally, we suggest how this inhibition may play a role in cell volume regulation in the proximal tubule.

Materials and Methods

Preparation of Brush Border Membrane Vesicles

Renal brush border membrane vesicles were prepared from rabbit renal cortex as described (Soveral et al., 1997). After kidney decapsulation the whole process was conducted at a temperature of 4°C in the presence of a single buffer containing 16 mM mannitol, 2 mM Tris-Hepes pH 7.4 (final osmolarity 18 mosM).

Other vesicle preparations with different internal solute concentrations were obtained by replacing the 16 mM mannitol buffer by other mannitol buffers with different osmolarities or with cellobiose buffer (18 or 85 mosM).

Protein content was determined using the Bradford technique (Bradford, 1976) with bovine albumin as standard.

Enrichment in specific activity (BBMV/crude homogenate) of the apical (leucine-aminopeptidase and alkaline phosphatase) and basolateral (Na^+/K^+ ATPase and K^+-stimulated phosphatase) enzyme markers, as well as the contamination by the lysosomal fraction (acid phosphatase activity) was described in our companion paper (Soveral et al., 1997).

The membrane preparations obtained were either immediately used for experiments, or stored in liquid nitrogen for later use.

Osmolarity Measurements

All solution osmolarities were determined from freezing point depression on a cryometric automatic semi-micro osmometer (Knauer GmbH, Germany). Standards of 100 and 400 mosM were analyzed prior to samples, which were measured in triplicate.

Identification of the CHIP28 Protein

Western analysis was performed as described previously (Towin, Staehelin & Gordon, 1979) with minor modifications. BBMV prepared in 18 mosM mannitol buffer and RBC hemoglobin-free membranes (Bennett, 1983) were used. After the electrophoresis through a 12% polyacrylamide gel containing SDS, with a stacking gel of 5%, using a discontinuous buffer system (Laemmli, 1970), the samples were transferred to a nitrocellulose filter (BA85, Schleicher & Schuell) on a Trans-Blot-SD (BioRad) by applying 15V–1 hr. After blockage and washing, the blots were incubated with 0.1 ml cm^{-2} of affinity-purified anti-28 KDa IgG (kindly given by P. Agre, Johns Hopkins University School of Medicine, Baltimore, MD). The antiserum was used at a dilution of 1/400 on immunoblots. The visualization was performed by ECL (Amersham).

Both preparations of RBC hemoglobin-free membranes and BBMV showed a band corresponding to a 28 KDa protein reactive to the antiserum anti-CHIP28. These results indicate that our BBMV preparations contain CHIP28 protein, a result also obtained by other authors (Denker et al., 1988).

Vesicle Size Determination

Vesicle size of all the membrane preparations was determined by QELS and vesicle trapped volume measurements, as described (Soveral et al., 1997). These two methods were used to determine the equilibrium volumes of vesicles prepared in 18 and 85 mosM cellobiose buffers, and subjected to several osmotic shocks. The results of both methods were in good agreement (*see* Fig. 4 of Soveral et al. (1997)).

Stopped-Flow Experiments

Experiments were performed on a HI-TECH Scientific PQ/SF-53 stopped-flow apparatus, which has a 2 msec dead time, temperature controlled, interfaced with an IBM PC/AT compatible 80386 microcomputer. Unless otherwise specified, experiments were done at 23°C. Three runs were usually stored and analyzed in each experimental condition. In each run 0.1 ml of vesicles (0.4 mg protein/ml) prepared with the desired osmotic buffer, was mixed with an equal amount of hyperosmotic mannitol or cellobiose solutions to reach different inwardly directed gradients of solute. The time course of 90° scattered light intensity at 400 nm was followed for 8 sec and 0.3 sec simultaneously in two channels, with an acquisition rate of 0.2 and 3 KHz respectively.

Results

Dependence of the Total Change in Light Scatter Intensity on the Tonicity of the Osmotic Shock

To minimize the signal-to-noise ratio (Meyer & Verkman, 1987; van der Goot et al., 1989*a;* van Hoek et al., 1990), vesicles were prepared in low osmolarity buffers. Figure 1 shows records of a typical stopped-flow experiment where the light scatter intensity from a vesicle suspension prepared in 18 mosM cellobiose buffer and suddenly exposed to different hyperosmotic solutions, was followed for 8 sec. The different curves are identified by

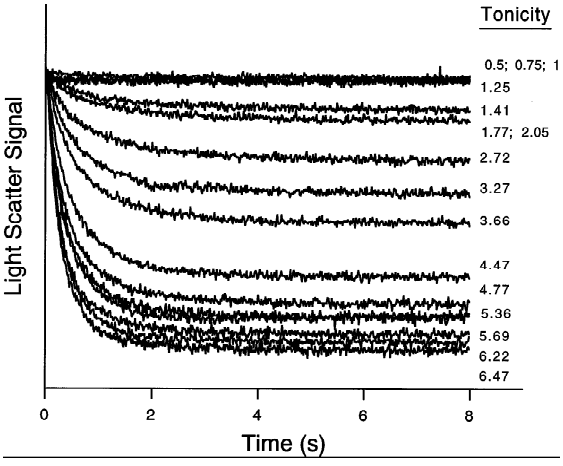

Fig. 1. Record of a typical stopped-flow experiment where the light scatter intensity $I(t)$ from a vesicle suspension equilibrated in 18 mosM cellobiose solution was suddenly exposed to different osmotic shocks. Data acquisition was followed for 8 sec at 0.2 KHz.

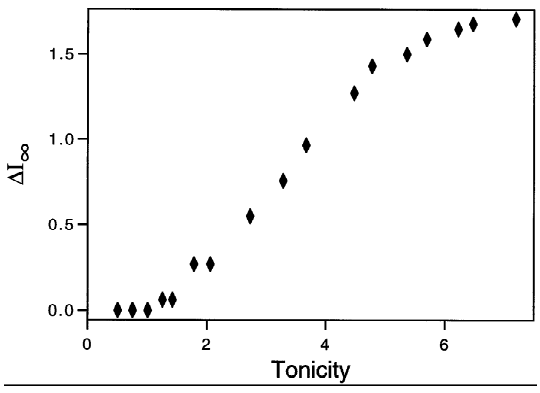

Fig. 2. Total light scatter intensity ($\Delta I_\infty = I_o - I_\infty$) as a function of tonicity of the osmotic shock, obtained from the records of Fig. 1.

the tonicity of the shock, Λ, defined as the ratio of the final to initial osmolarity of the outside medium, i.e., $\Lambda = (osm_{out})_\infty/(osm_{out})_0$. Identical results were obtained when mannitol was used instead of cellobiose.

Figure 2 shows the nonlinear dependence of the total change in light scatter intensity ($(\Delta I)_\infty = I_o - I_\infty$) with Λ, obtained by analyzing the stopped flow signals of Fig. 1. This sigmoidal curve shows two tonicity domains, $\Lambda < 1$ and $\Lambda > 6$, where the light scatter signal does not detect any volume changes. Indeed, for $\Lambda < 1$, an increase in vesicular volume was expected if an influx of water occurs, whereas for $\Lambda > 6$ a further decrease in volume should occur if there was no minimum volume shrinkage.

Osmotic Behavior of Vesicles

In a vesicle suspension, the total concentration of solutes inside the vesicles equals the total inner osmolarity osm_{in} and is the sum of the concentrations of the impermeant species (*S*) used in the buffer preparation and of any other species (*NS*) that remained inside the vesicles during the preparation. If the solute *S* is the only solute species of the external medium, than its concentration equals the medium osmolarity, ($osm_{out} = C_{S\,out}$). If these vesicles of volume V are subjected to an osmotic shock with the same impermeant solute *S*, then the osmotic water flow J_v that crosses the vesicle membrane of area A can be related to the change in vesicular volume by:

$$-\frac{dV}{Adt} = J_v = P_f \overline{V}_w \left(\frac{\Delta P - \Delta\Pi}{RT}\right) \qquad (1)$$

where P_f is the osmotic permeability coefficient, V_w is the partial molar volume of water, $\Delta P = (P_{in} - P_{out})$ and $\Delta\Pi = RT(osm_{in} - osm_{out})$ are the hydrostatic and osmotic pressure differences between the inside and the outside of the vesicles. Substituting the inner and outer osmolarities and considering the initial vesicular volume as V_o, then Eq. (1) can be rearranged to give:

$$\begin{aligned} d\frac{V}{V_o}/dt &= P_f \frac{A}{V_o} \overline{V}_w \left((osm_{in} - osm_{out}) - \frac{\Delta P}{RT}\right) \\ &= P_f \frac{A}{V_o} \overline{V}_w \left((C_{S\_in} + C_{NS\_in} - osm_{out}) - \frac{\Delta P}{RT}\right) \end{aligned} \qquad (2)$$

where $C_{S\,in} + C_{NS\,in}$ represents the sum of the osmolar concentrations of impermeable solutes within the vesicle at any time (subscript *S* denotes contribution of solutes in the preparation buffer, while *NS* denotes all other solutes). Since the solutes are impermeable, it follows that $V(C_{S\,in} + C_{NS\,in})$ is a constant equal to the total number of internal osmoles at any time. Let the subscript *o* refer to initial values. Then, using expressions for $C_{S\,in}$ and $C_{NS\,in}$ obtained from Eq. (8) and (11) of Soveral et al. (1997), we have

$$\begin{aligned} C_{S\_in} + C_{NS\_in} &= \frac{V_o((C_{S\_in})_o + (C_{S\_in})_o)}{V} \\ &= \frac{V_o\left((osm_{out})_o + \dfrac{(\Delta P)_o}{RT}\right)}{V} \end{aligned} \qquad (3)$$

The empirical dependence of ΔP on V is also obtained from Eq. (13) of Soveral et al. (1997) by substituting V for V_∞ and ΔP for $(\Delta P)_\infty$ i.e.,

$$\frac{(\Delta P)}{RT} = \frac{(\Delta P)_{max}}{RT}\left(1 - \frac{\left(\frac{V_o}{V}\right)^n}{c^n + \left(\frac{V_o}{V}\right)^n}\right) \qquad (4)$$

where ΔP_{max}, c, and n are parameters that can be estimated by the experimental results as indicated by Soveral et al. (1997). Inserting (3) and (4) into (2), we arrive at

$$\frac{d\frac{V}{V_o}}{dt} = P_f \frac{A}{V_o}\overline{V}_w \left(\left(\frac{V_o\left((osm_{out})_o + \frac{(\Delta P)_o}{RT}\right)}{V} - osm_{out}\right) - \frac{(\Delta P)_{max}}{RT}\left(1 - \frac{\left(\frac{V_o}{V}\right)^n}{c^n + \left(\frac{V_o}{V}\right)^n}\right)\right) \qquad (5)$$

a differential equation in the single variable V which describes the kinetics of water transport in response to an osmotic shock. With the exception of P_f, all of the constants in Eq. (5) can be determined independently of these kinetics. It follows that P_f can be estimated by numerically integrating Eq. (5) with different values of P_f and comparing the numerical results with empirical data obtained from osmotic shock experiments. To accomplish this with light scattering measurements requires careful calibration of scattering signal to vesicle volume.

Relation Between Change in Vesicular Volume and Light Scattering Signal

The precise relation of light scatter intensity measured by conventional stopped flow spectrophotometers to vesicular volume is complex, device dependent, and is generally approximated by some arbitrary empirical function. Some authors arrange their setup so that the photomultiplier output increases with scattered light while others prefer to have the signal increase with vesicular volume, and arrange for a decreased output with increased scattered light. In view of the above, it is not surprising that there is no general agreement on an optimal empirical calibration function.

We have tried three different functions: (i) the relation used by Pratz et al. (1986) (ii) a linear relation between vesicular volume V/V_o and output signal I (Verkman, Dix & Seifter, 1985*a*), and (iii) a linear relation between V/V_o and the reciprocal of the output, *1/I*. In our hands, the relation used by Pratz et al. (1986) was highly nonlinear throughout the working range of volumes and was accordingly discarded. The other two both fit the calibration data within a limited but workable range ($V/V_o > 0.6$), however the latter,

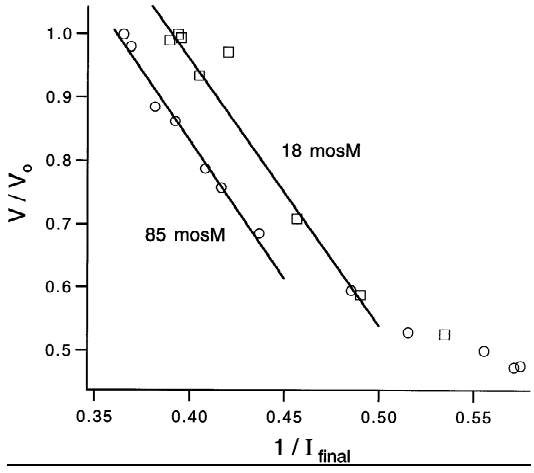

Fig. 3. Change of vesicular volume (V/V_o) as a function of the reciprocal final light scatter intensity. Vesicles prepared in 18 or 85 mosM cellobiose buffer were subjected to different osmotic shocks.

$$\frac{V}{V_o} = a\frac{1}{I} + b \qquad (6)$$

with a and b constant, was adopted because it gave more consistent results when comparing data on vesicles prepared in different media. These are shown in Fig. 3 where light scatter data has been taken from Fig. 1 and the volume corresponding to the same tonicity is taken from Fig. 4. Both sets of data (18 and 85 mosM) were obtained from the same batch of vesicles.

Knowing that the relation between V and $1/I$ is linear, allows us to obtain separate calibrations for each stopped flow trace. For any given trace with known tonicity, the initial I corresponding to $V/V_o = 1$, and final I corresponding to V/V_o obtained from Fig. 4, are used to calculate a and b of Eq. (6). Failure to account for the nonlinear relation between reciprocal volume and tonicity as shown in Fig. 4 can result in significant calibration errors.

Osmotic Permeability Coefficients

Permeability coefficients were estimated as indicated above. The A/V_o ratio used was calculated using the diameters measured by QELS for each vesicle population ($\phi = 373 \pm 16$ and 360 ± 20 nm for the 18 and 85 mosM respectively), assuming a spherical shape.

Figure 5 presents an example of BBMV prepared in

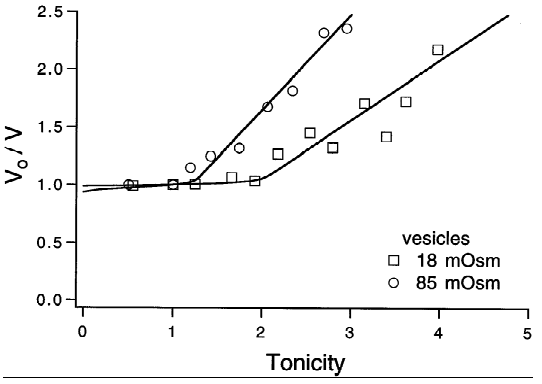

Fig. 4. Equilibrium volume ratio V_o/V_∞ of BBMV subjected to osmotic shocks of different amplitudes, as a function of the tonicity of the shock. Equilibrium volumes were measured by trapped volumes. BBMV were prepared in 18 and 85 mosM cellobiose buffers (data redrawn from Fig. 4 of Soveral et al. 1997).

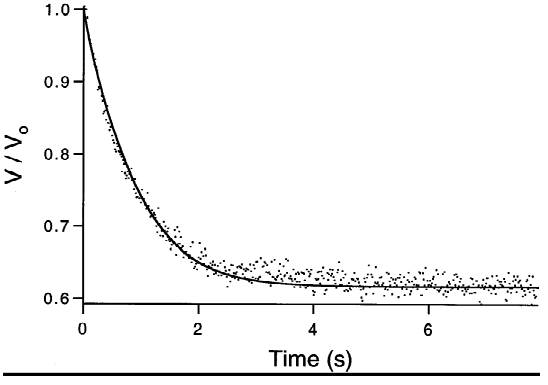

Fig. 5. Fit of a calibrated volume signal of BBMV prepared in 18 mosM cellobiose buffer and subjected to an osmotic shock of tonicity 3.3. The calculated P_f value was 3.2×10^{-3} cm sec^{-1}.

18 mosM buffer and subjected to an osmotic shock of tonicity 3.3. The calculated P_f values was 3.2×10^{-3} cm sec^{-1}. Table 1 show the results of vesicles prepared in 18 and 85 mosM buffer.

Higher P_f values were obtained for vesicles treated with the channel former Gramicidin A (10 and 20 μg/mg protein) as described (Worman & Field, 1985). An increase of 25% to 40% of P_f control values were obtained respectively for the lower and higher Gramicidin A concentration.

P_f inhibition of 52% was found for vesicles incubated for 30 min at room temperature with 10 or 15 mM pCMBS, after taking their respective V_o/A ratio into account. However, when compared with the control value (ϕ = 370 nm), a decrease in initial vesicle diameter was observed (ϕ = 230 nm). This large change in initial volume casts doubt about the condition of these vesicles at these pCMBS concentrations.

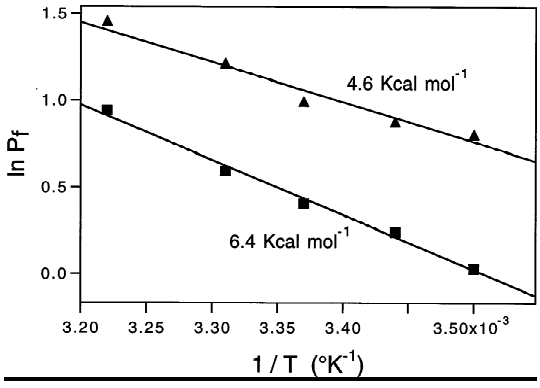

Fig. 6. Activation energy determination of water transport. BBMV prepared in 18 mosM mannitol buffer equilibrated at different temperatures, were subjected to different osmotic shocks. The activation energies obtained were 6.4 Kcal mol^{-1} for low tonicity shocks (1.52) and 4.6 Kcal mol^{-1} for higher tonicities (2.25, 2.59, 2.88, 3.22).

Activation Energy Measurements

The activation energy for water transport was estimated from a plot of ln P_f *vs. 1/T*. Figure 6 shows two plots with activation energies equal to 4.6 and 6.4 Kcal mol^{-1} for vesicles prepared in 18 mosM buffer. The higher value 6.4 was obtained with a low tonicity shock (1.52) that characteristically yields unusually low P_f values (*see* Table 1 for 18 mosM vesicles). The other value, 4.6, was obtained by averaging all values obtained for higher tonicities (2.25, 2.59, 2.88, 3.22) which have P_f values that generally agree with each other.

Lag Time is Related to the Dissipation of the Hydrostatic Pressure Difference

In addition to influencing the driving force for transport, ΔP appears to be related to an anomaly seen in the early transport kinetics shown in detail in Fig. 7. Here an initial delay of osmotic shrinkage, the lag time, corresponding to a very small change in initial volume is apparent. Very small initial volume changes are also associated with the dissipation of the initial hydrostatic pressure (Soveral et al., 1997). In addition, both the time lag and the internal pressure dissipation are prolonged in the lower tonicity ranges. These correlations suggest a causal relation between the two. Further evidence is provided by the experiment illustrated in Fig. 9.

Here control vesicles prepared in 22 mosM cellobiose buffer and subjected to an osmotic shock of tonicity 2.6, are compared with similar vesicles subjected to the same final osmotic shock but given in two consecutive steps. In the first step, vesicles are preshrunk by a first osmotic shock (Λ = 1.7)—enough to dissipate partially or totally the hydrostatic pressure gradient. In the second step these preshrunk vesicles are subjected to a second

Table 1. P_f values obtained in vesicles prepared in 18 and 85 mosM buffer. P_f is expressed in cm $sec^{-1} \times 10^3$

18 mosM		85 mosM	
Λ	P_f (cm $sec^{-1} \times 10^3$)	Λ	P_f (cm $sec^{-1} \times 10^3$)
1.41	1.7	1.244	3.62
2.055	2.30	1.291	3.62
2.722	3.99	1.464	4.4
3.277	3.99	1.541	3.95
3.666	3.55	1.732	4.29

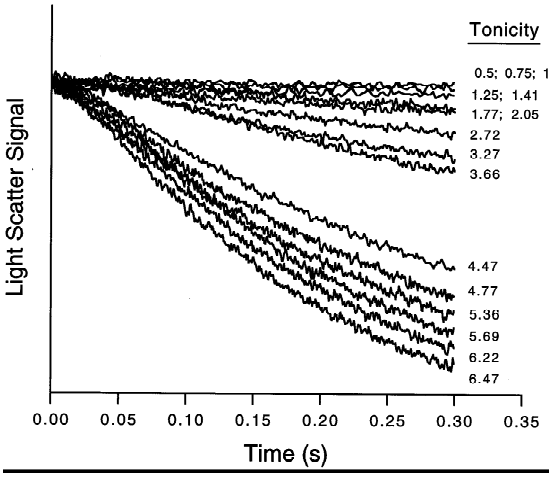

Fig. 7. Record of a typical stopped flow experiment where the light scatter intensity $I(t)$ from a vesicle suspension equilibrated in 18 mosM cellobiose solution was suddenly exposed to different osmotic shocks. Data acquisition was followed for 0.3 sec at a frequency of 3 KHz.

shock ($\Lambda = 1.55$). The total change in light scatter signal obtained by the two consecutive shocks equals the magnitude obtained by the single 2.6 tonicity osmotic shock; both vesicle populations reach the same final volume. Figure 8 shows that the time lag, characteristic of control vesicles (upper curve), disappears when the similar vesicles are preshrunk ($\Lambda = 1.7$) and then subjected to a second osmotic shock ($\Lambda = 1.5$, lower curve). This behavior can be explained if we consider that the dissipation of the initial hydrostatic pressure difference has already occurred during the first step.

The experiment provides evidence that this pressure is the primary cause of the lag time. This experiment also provides evidence that the time lag is not due to an artifact introduced by the stopped flow-light scattering device (e.g., unstirred layers, hydrodynamic mixing transients picked up by the photomultiplier, vibrations, etc.) nor is it due to improper calibration of the light scattering signal. Although the pressure and associated lag time is seen most easily in vesicles prepared in 18 mosM buffer they are also present in higher mosM buffer preparations. Evidence for the same pressure volume dependence in

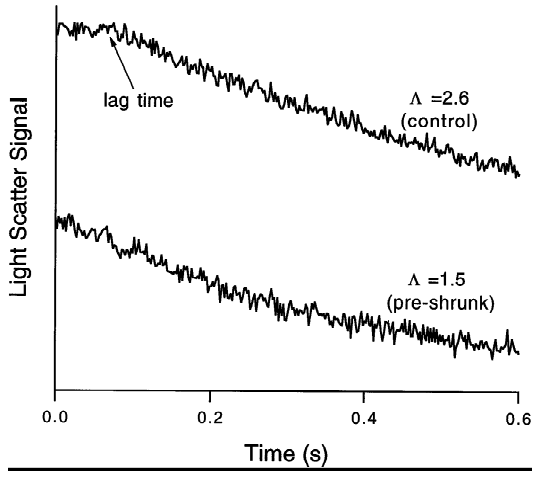

Fig. 8. Light scatter signals obtained with BBMV prepared in 22 mosM cellobiose buffer and subjected to different osmotic shocks. In the upper trace, where a ''lag time'' can be observed, control vesicles were subjected to an osmotic shock of tonicity 2.6. In the lower trace, vesicles were first preshrunk by an osmotic shock ($\Lambda = 1.7$) sufficient to dissipate the initial hydrostatic pressure difference and were then subjected to a second osmotic shock with a magnitude that would cause the vesicles to reach the same final vesicular volume as the non preshrunk vesicles ($\Lambda = 1.55$, lower trace). In this curve, the ''lag time'' completely disappears. The *y* axis has an offset.

the 85 mosM preparation is shown in Fig. 6 of Soveral et al. (1997). Lag times are also present in the 85 mosM preparation but they are much shorter because the larger absolute values of osmotic shock gradients used in these experiments dissipates the pressure much faster.

Lag Time Corresponds to a Lower Permeability Coefficient

During the lag time the vesicular volume responds very slowly despite the presence of a significant difference in chemical potential of water across the membrane. This implies that the water permeability is reduced during this time. We have shown that the time lag is (i) present when the inferred hydrostatic pressure is present, and (ii) disappears when the pressure is removed. Further, both pressure and lag time are more prominent at lower tonicities. Thus, it is reasonable to propose that the internal hydrostatic pressure inhibits vesicular water permeability.

To pursue the labile water permeability, we have reanalyzed the data assuming two discrete permeabilities: during the lag time $P_f = P_{fslow}$ and beyond the lag time $P_f = P_{ffast}$. Transition from one permeability to the other is assumed to occur when V reaches a critical volume V_{crit}. Values of P_{fslow}, P_{ffast}, and V_{crit}, optimized to give best fits to the data (*see* Fig. 9), are shown in Table 2 for shocks that are large enough to completely dissipate

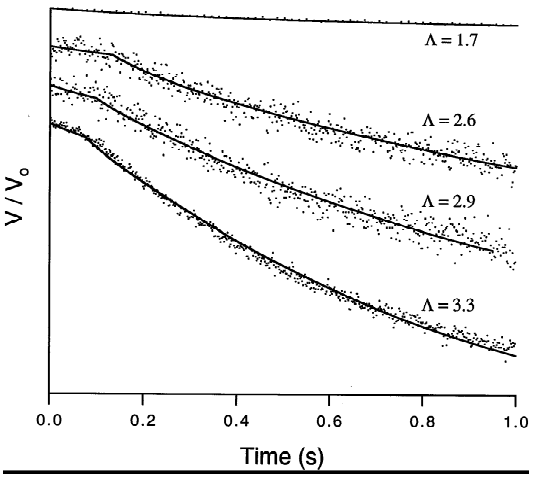

Fig. 9. First second of volume change in BBMV prepared with 18 mosM cellobiose buffer and subjected to four different osmotic shocks. The values of P_{fslow}, V_{crit}, and P_{ffast} were obtained fitting the data to Eq. (5). Data shown by dots and fitted curves by solid lines.

the hydrostatic pressure. In Table 2, the values of P_{ftotal} were obtained from the 8-sec curves, ignoring the existence of the lag time and assuming a single P_f value.

Data presented in Table 2 show that the values of P_{ffast} and P_{ftotal} are similar for the different files analyzed, and should correspond to a permeability where the contribution of activated channels is maximum. The P_{fslow} values are different. For expediency, we have assumed an abrupt transition in permeabilities at some critical volume. However if hydrostatic pressure is indeed responsible for the lowering of water permeability we would expect P_f to be some continuous function of pressure starting at a minimum value limited by lipid bilayer permeability, where no channels are active, reaching its maximum value, P_{ffast}, asymptotically when all the pressure has been dissipated. In this case P_{fslow} may represent some weighted average of different states of channel activation. Perhaps the simplest example of the continuum is provided by the case where channel inhibition decays exponentially with permeability i.e.,

$$P_f = P_{ffast} - k\left(1 - e^{\left(-\lambda \frac{\Delta P}{RT}\right)}\right) \qquad (7)$$

where P_{ffast}, k and λ are constants to be determined by curve fitting. When $\Delta P = 0$, then $P_f = P_{ffast}$ (same as before). Figure 10*A* and *B* compares this simple example of a continuum with the discrete transition assumption. It shows curves fit to the data points: (*A*) the permeability jump at V_{crit}, and (*B*) the continuous increase of P_f with the decrease of the hydrostatic pressure. Both approaches give similar P_{ffast}. However, as expected, the P_{fslow} value obtained by the permeability jump approach is higher than the minimum P_f value ($P_{f\_min} = 0.43 \times 10^{-3}$ cm sec^{-1}) obtained with the continuous permeability approach.

Discussion

Vesicle preparations containing the water channel protein CHIP28, show a nonlinear behavior of the total change in light scatter intensity with the tonicity of the osmotic shock (Fig. 2). Similar nonlinearities were observed for the dependence of volume ratio V_o/V with Λ (Fig. 5). These are presumed to be due to an imbalance of nondiffusible solute osmolarity across the vesicle membrane which is counterbalanced by a hydrostatic pressure difference that maintains the membrane under strain (Soveral et al., 1997). When confronted by a hypertonic shock the vesicle shrinks and dissipation of the hydrostatic pressure can be anticipated.

Evidence for the existence the internal hydrostatic pressure was provided in our earlier paper (Soveral et al., 1997) where it explained: (i) the influx of mannitol that follows an osmotic shock, (ii) the nonlinear dependence of volume on the reciprocal tonicity, (iii) the dependence of the volume changes on the preparation buffer osmolarity, (iv) a Donnan ratio that departs significantly from unity. More importantly, the inferred hydrostatic pressure led to an estimate of an elastic modulus which agreed with those cited in the literature for similar systems.

In the face of a hypertonic shock there is a significant lag time before the maximal vesicular volume response (dV/dt) sets in. The lag time does not appear to be an artifact introduced by the stopped-flow device or its associated optics. In addition, it cannot be due to heterogeneities in the permeability or the size of the vesicle population. If it were, then the early trace of the volume curve would have a positive curvature; in fact it is negative. We conclude that the lag time corresponds to a period of reduced water permeability. This reduction is related to the inferred hydrostatic pressure because the time lag is present when the pressure is present and disappears when the pressure is removed.

A variable water permeability complicates the analysis of osmotic shock data. The naive, and perhaps most prudent, approach is to examine the data piecewise, assuming an average constant permeability during the slow lag, along with a separate constant permeability following the lag. The data is easily fit by this simple strategy. More likely the water permeability is a continuous, but unknown, function of pressure. Assuming a simple exponential dependence of P_f on pressure, also fits the data. In either case, following dissipation of pressure, our permeability estimates yield similar permeability values of the order of 4×10^{-3} cm sec^{-1}. This is somewhat lower than values reported in the literature for BBMV and requires discussion.

Table 2. Lag time, critical volume and respective P_f values for the fast and slow components of the shrinking curves, and P_{ftotal} calculated from the total trace (8 sec)

Tonicity (Λ)	Lag time (msec)	V_{crit}	P_{fslow} (cm sec^{-1} × 10^3)	P_{ffast} (cm sec^{-1} × 10^3)	P_{ftotal} (cm sec^{-1} × 10^3)
2.6	133	0.989	0.81	4.6	4.1
2.9	98	0.983	1.27	4.46	4.0
3.3	73	0.985	1.45	4.86	3.9

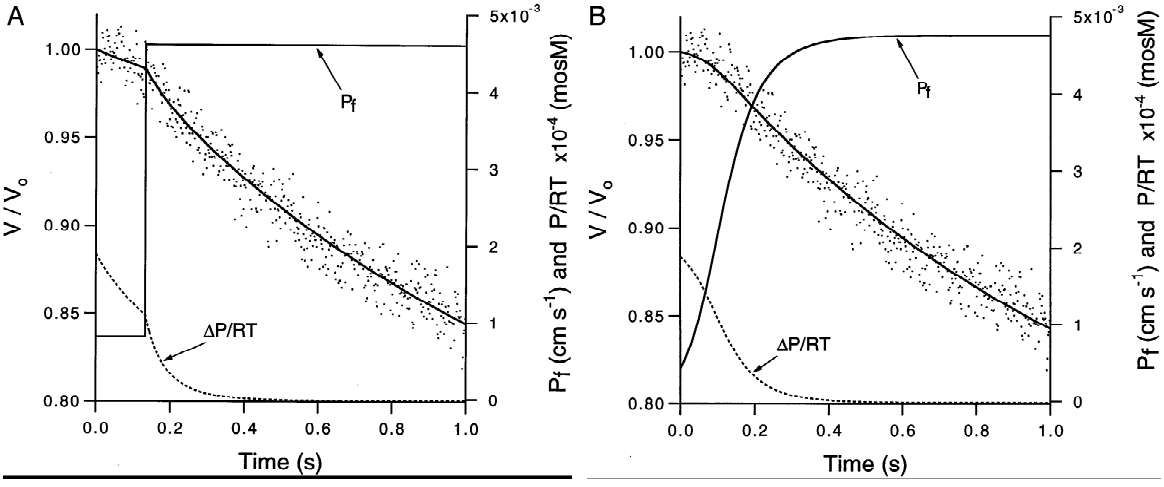

Fig. 10. P_f and hydrostatic pressure dependence on the vesicular volume for vesicles prepared in 18 mosM cellobiose buffer subjected to a 2.6 tonicity osmotic shock. Both panels show the curve fit to the data points by (*A*) a hypothetical permeability jump at V_{crit}, and (*B*) a hypothetical continuous increase of P_f, with the decrease of the hydrostatic pressure. Data shown by dots and fitted curves by solid lines.

Values of P_f ranging all the way from 7.3 to 60.0 × 10^{-3} cm sec^{-1} have been reported by a variety of laboratories (Verkman et al., 1985*a,b;* van Heeswijk & van Os, 1986; Pratz et al., 1986; Verkman & Ives, 1986; Meyer & Verkman, 1987; Pratz, Ripoche & Corman, 1987; van der Goot et al., 1989*a,b;* Sabolic et al., 1992). Methods of data analysis have varied; some authors fit their data to a single exponential, others to a double exponential. Single exponential fits have a theoretical basis provided that the volume perturbation is small, a criterion that is technically difficult to fulfill when working with vesicles as small as BBMV. Double exponential fits may reflect two populations, or it may simply obscure the basic nonlinearity that occurs in larger volume perturbations. Still other authors have estimated permeability from a single initial derivative of the light scattering signal, a procedure that we have not found successful, especially in the face of a lag time. Only one laboratory appears to have taken the entire volume curve into account, retrieving their parameters from fitting a basic theoretical model to the data without approximations. Their reported permeability value for rabbit BBMV is 7.3 × 10^{-3} cm sec^{-1} at 23°C (11 × 10^{-3} cm sec^{-1} at 37°C) (Verkman et al., 1985*a;* Meyer & Verkman, 1987). They did not report a nonlinearity in the calibration curve of *V vs. 1/*Λ nor did they introduce hydrostatic pressure into their kinetic model. It is not clear whether this would account for the difference.

Some credibility is lent to our results by considering activation energies. Our value of 4.6 kcal mol^{-1} compares very favorably with the 4–5 kcal mol^{-1} reported for water channels in red cells and for diffusion and bulk flow of water in water (Wang, Robinson & Edelman, 1953; Farmer & Macey, 1970; Vieira, Sha'afi & Solomon, 1970; Foster, 1971; Macey, Karan & Farmer, 1972). The estimate of 6.4 kcal mol^{-1} for low osmotic tonicity shocks is also reasonable. In these vesicles the lag time, where channel permeability is low, occupies a greater proportion of the shrinkage curve. Thus the contribution of water transport with a large activation energy through lipid pathways plays a more prominent role and skews the measured energy toward higher values.

Other estimates of activation energies are not as easy to interpret. Meyer & Verkman (1987) reported a biphasic response, with a sudden break at $T = 33°$, yielding $E_A = 2.8$ kcal mol^{-1} for $T < 33°$ and $E_A = 13.7$ kcal mol^{-1} for $T > 33°$. Van Heeswijk & van Os (1986) claim an activation energy of 1.0 kcal mol^{-1}. These estimates are significantly below activation energies of water interacting with water in bulk flow or diffusion and would

seem to imply a truly catalytic action of the channels on water transport, an interpretation we are not inclined to pursue. Further, the apparent break in the Arrhenius plot obtained by Meyer & Verkman (1987) cannot be interpreted as due to a composite of water channels with the lower (2.8 kcal mol^{-1}) activation energy, and lipid pathways with the higher energy showing up more prominently at higher temperatures. If we assume any reasonable ratio of channel to lipid permeability and construct a plot resulting from sum of the two processes with assumed activation energies of 2.8 and 13.7 kcal mol^{-1}, we arrive at a figure which is fairly linear with no apparent break and with the slope in the higher temperature region less than required for a 13.7 kcal mol^{-1} process. If we fit a two process model to their data we arrive at two activation energies; one is much smaller than 2.8, the other considerably larger than 13.7 kcal mol^{-1}.

The low permeabilities as well as the pressure inhibition of water transport were unanticipated. Estimated values of the pressure may also seem high, but, for a given surface tension, this results from their small radius. As shown in Soveral et al. (1997) the strain and area expansion of these vesicles at the point of rupture is similar to that measured in other larger cells. It is likely that the more direct cause of the inhibition of water transport arises from pressure induced membrane strain. Thus larger intact cells would be subject to similar inhibitions even though the pressure that initiate the strain is hardly discernible.

The physiological significance of these findings, if any, is probably connected with the huge fluid reabsorption in the proximal tubule which accompanies transport of essential solutes. Because solute reabsorption is so massive, small fluctuations of transport rates between brush border and basal lateral membranes could lead to large intracellular accumulations of fluid. A low permeability of the apical membranes which will tend to shunt water reabsorption through extracellular transjunctional pathways would make cellular volume transients easier to regulate. If fluid does accumulate within the cell, it could lead to increased membrane strain which would inhibit apical membrane water flux. Because of geometrical differences there is no reason to assume the same strain would appear in the basolateral membrane, and assuming an equivalent inhibition of the basolateral membrane does not occur, then the cell volume would diminish. Thus the presence of water channels in the apical membrane with distinct properties could serve as a volume and/or pressure regulator. The credibility of these speculations will require similar studies on both apical and basolateral membranes under more physiological conditions as techniques evolve.

We would like to thank Professor P. Agre for supplying the antibody anti-CHIP28, and Professor G. Ribeiro for the execution of the immunoblot techniques. We thank the Junta Nacional de Investigação Científica e Tecnológica for financial support and the Instituto de Tecnologia Química e Biológica, Universidade Nova de Lisboa, for a Visiting Professorship to R.I. Macey.

This work was supported by a grant from Junta Nacional de Investigação Científica e Tecnológica, Portugal JNICT SAU/757/90.

References

Bennett, V. 1983. Proteins involved in membrane's cytoskeleton association in human erythrocytes: spectrin and ankyrin, and Band3. *Meth. Enzymol.* **96:**313–324

Bradford, M. 1976. A rapid and sensitive method for the quantitation of microgram quantities of protein utilizing the principle of protein-dye binding. *Anal. Biochem.* **72:**248–254

Denker, B.M., Smith, B.L., Kuhajda, F.P., Agre, P. 1988. Identification, purification, and partial characterization of a novel M_r 28,000 integral membrane protein from erythrocytes and renal tubules. *J. Biol. Chem.* **263:**15634–15642

Donowitz, M., Emmer, E., McCullen, J., Reinlib, L., Cohen, M.E., Rood, R.P., Madara, J., Sharp, G.W.G., Murer, H., Malmstrom, K. 1987. Freeze-thaw and high-voltage discharge allow macromolecule uptake into ileal brush-border vesicles. *Am. J. Physiol.* **252:**G723–G735

Evers, C., Haase, W., Murer, H., Kinne, R. 1978. Properties of brush border vesicles isolated from rat kidney cortex by calcium precipitation. *Memb. Biochem.* **1:**203–219

Farmer, R.E.L., Macey, R.I. 1970. Perturbation of red cell volume: rectification of osmotic flow. *Biochim. Biophys. Acta* **196:**53–65

Foster, R.E. 1971. The transport of water in erythrocytes. *Current Topics in Membrane Transport* **2:**41–98

Laemmli, U.K. 1970. Cleavage of structural proteins during the assembly of the head of bacteriophage T4. *Nature* **227:**680–685

Macey, R.I. 1984. Transport of water and urea in red blood cells. *Am. J. Physiol.* **246:**C195–C203

Macey, R.I., Karan, D.M., Farmer, R.E.L. 1972. Properties of water channels in human red cells. *In:* Biomembranes 3, F. Kreuzer and J.F.G. Slegers, editors. pp. 331–340. Plenum Publishing, New York

Meyer, M.M., Verkman, A.S. 1987. Evidence for water channels in renal proximal tubule cell membranes. *J. Membrane Biol.* **96:**107–119

Pratz, J., Ripoche, P., Corman, B. 1986. Evidence for proteic water pathways in the luminal membrane of kidney proximal tubule. *Biochim. Biophys. Acta* **856:**259–266

Pratz, J., Ripoche, P., Corman, B. 1987. Cholesterol content and water and solute permeabilities of kidney membranes from aging rats. *Am. J. Physiol.* **253:**R8–R14

Preston, G.M., Agre, P. 1991. Isolation of the cDNA for erythrocyte integral membrane protein of 28-Kilodaltons-member of an ancient channel family. *Proc. Natl. Acad. Sci. USA* **88:**11110–11114

Rigler, M.W., Ferreira, G.C., Patton, J.S. 1985. Intramembranous particles are clustered on microvillus membrane vesicles. *Biochim. Biophys. Acta* **816:**131–141

Sabolic, L.G., Valenti, G., Verbavatz, J.M., van Hoek, A.N., Verkman, A.S., Ausiello, D.A., Brown, D. 1992. Localization of the CHIP28 water channel in rat kidney. *Am. J. Physiol.* **263:**C1225–C1233

Solomon, A.K. 1989. Water channels across the red blood cell and other biological membranes. *Methods Enzymol.* **173:**192–222

Soveral, G., Macey, R.I., Moura, T.F. 1997. Mechanical properties of brush border membrane vesicles from kidney proximal tubule. *J. Membrane Biol.* **158:**

Towin, H., Staehelin, T., Gordon, J. 1979. Electrophoretic transfer of proteins from polyacrylamide gels to nitrocellulose sheets: proce-

dure and some applications. *Proc. Natl. Acad. Sci. USA* **76:**4350–4354

Van der Goot, F.G., Podevin, R.A., Corman, B.J. 1989*a*. Water permeabilities and salt reflection coefficients of luminal, basolateral, and intracellular membrane vesicles isolated from rabbit kidney proximal tubule. *Biochim. Biophys. Acta* **986:**332–340

Van der Goot, F.G., Ripoche, P., Corman, B.J. 1989*b*. Determination of solute reflection coefficients in kidney brush border membrane vesicles by light scattering: influence of refractive index. *Biochim. Biophys. Acta* **979:**272–274

Van Heeswijk, M.P.E., van Os, C.H. 1986. Osmotic water permeabilities of brush border and basolateral membrane vesicles from rat renal cortex and small intestine. *J. Membrane Biol.* **92:**183–193

Van Hoek, A., Jong, M., van Os, C.H. 1990. Effects of dimethylsulfoxide and mercurial sulphydryl reagents on water and solute permeability of rat kidney brush border membranes. *Biochim. Biophys. Acta* **1030:**203–210

Verkman, A.S. 1992. Water channels in cell membranes. *Annu. Rev. Physiol.* **54:**97–108

Verkman, A.S., Dix, J.A., Seifter, J.L. 1985*a*. Water and urea transport in renal microvillus membrane vesicles. *Am. J. Physiol.* **248:**F650–F655

Verkman, A.S., Dix, J.A., Seifter, J.L., Skorecki, K.L., Jung, C.Y., Ausiello, D.A. 1985*b*. Radiation inactivation studies of renal brush border water and urea transport. *Am. J. Physiol.* **249:**F806–F812

Verkman, A.S., Ives, H.E. 1986. Water permeability and fluidity of renal basolateral membranes. *Am. J. Physiol.* **250:**F633–F643

Vieira, F.L., Sha'afi, R.I., Solomon, A.K. 1970. The state of water in human and dog red cell membranes. *J. Gen. Physiol.* **55:**451–466

Wang, J.W., Robinson, C.V., Edelman, I.S. 1953. Self-diffusion and structure of liquid water. III. Measurement of the self-diffusion of liquid water with H^2, H^3 and O^{18} as tracers. *J. Am. Chem. Soc.* **75:**466–470

Worman, H.J., Field, M. 1985. Osmotic water permeability of small intestinal brush border membranes. *J. Membrane Biol.* **87:**233–239